INTERNATIONAL JOURNAL OF CLIMATOLOGY
Int. J. Climatol. **26**: 1315–1337 (2006)
Published online 21 March 2006 in Wiley InterScience (www.interscience.wiley.com). DOI: 10.1002/joc.1314

CONSENSUS BETWEEN GCM CLIMATE CHANGE PROJECTIONS WITH EMPIRICAL DOWNSCALING: PRECIPITATION DOWNSCALING OVER SOUTH AFRICA

B. C. HEWITSON[a,*] and R. G. CRANE[b]

[a] *Climate System Analysis Group, Department Environmental and Geographical Science, University of Cape Town, Private Bag, Rondebosch 7701, South Africa*

[b] *Alliance for Earth Science, Engineering, Development in Africa, Earth and Mineral Science College, Pennsylvania State University, University Park, PA 16801, USA*

Received 8 June 2005
Revised 21 December 2005
Accepted 21 December 2005

ABSTRACT

This paper discusses issues that surround the development of empirical downscaling techniques as context for presenting a new approach based on self-organizing maps (SOMs). The technique is applied to the downscaling of daily precipitation over South Africa. SOMs are used to characterize the state of the atmosphere on a localized domain surrounding each target location on the basis of NCEP 6-hourly reanalysis data from 1979 to 2002, and using surface and 700-hPa u and v wind vectors, specific and relative humidities, and surface temperature. Each unique atmospheric state is associated with an observed precipitation probability density function (PDF). Future climate states are derived from three global climate models (GCMs): HadAM3, ECHAM4.5, CSIRO Mk2. In each case, the GCM data are mapped to the NCEP SOMs for each target location and a precipitation value is drawn at random from the associated precipitation PDF. The downscaling approach combines the advantages of a direct transfer function and a stochastic weather generator, and provides an indication of the strength of the regional *versus* stochastic forcing, as well as a measure of stationarity in the atmosphere–precipitation relationship.

The methodology is applied to South Africa. The downscaling reveals a similarity in the projected climate change between the models. Each GCM projects similar changes in atmospheric state and they converge on a downscaled solution that points to increased summer rainfall in the interior and the eastern part of the country, and a decrease in winter rainfall in the Western Cape. The actual GCM precipitation projections from the three models show large areas of intermodel disagreement, suggesting that the model differences may be due to their precipitation parameterization schemes, rather than to basic disagreements in their projections of the changing atmospheric state over South Africa. Copyright © 2006 Royal Meteorological Society.

KEY WORDS: climate change; downscaling; self-organizing maps; global climate model; precipitation; South Africa

1. INTRODUCTION

Empirical downscaling is a widely used technique for exploring the regional and local-scale response to global climate change as simulated by comparatively low-resolution global climate models (GCMs). As noted in the third assessment report (TAR) of the intergovernmental panel on climate change (IPCC, 2001), downscaling has wide appeal because of its low computational needs and its relative ease of application. This makes it particularly attractive to the impacts community and especially to developing nations, and the approach has been widely adopted. (See, e.g. the extensive references of the IPCC TGICA guidance document on statistical (empirical) downscaling, from http://ipcc-ddc.cru.uea.ac.uk/guidelines/index.html.) For regional climate change projections, the TAR also concludes that empirical approaches have similar skill levels as

* Correspondence to: B. C. Hewitson, Department of Environmental and Geographical Science, University of Cape Town, Private Bag, Rondebosch 7701, South Africa; e-mail: hewitson@egs.uct.ac.za

current implementations of numerical regional climate models (RCMs). While increasing in popularity, there has been little discussion of the advantages and, more importantly, the limitations in using empirical techniques for climate downscaling. In this paper we discuss the basic assumptions that underlie this approach and present a new technique that attempts to reduce these limitations in an empirical downscaling of daily precipitation over South Africa.

The TAR, however, also highlights the extensive and diverse list of empirical techniques that have been applied to climate downscaling (IPCC, 2001: Chapter 10, Appendix A), and the number has grown subsequent to the TAR publication. There has been little assessment of the strengths and weaknesses of the different methodological approaches. Many techniques are based on different statistical models, requiring different assumptions concerning the input data, and subjective decisions on the choice of statistical parameters. The outputs may be strongly dependent on the atmospheric variables and the period of observation used. In some respects, this has reduced clarity and confidence in the results, and limited the value of empirical downscaling for the policy and impacts community – a community urgently in need of credible regional-scale scenarios of future climate. Regional Climate Models, while often perceived by the impacts community as an optimum approach to downscaling GCMs, have their own problems in application. Most notable are the sensitivity and validation analyses necessary to select the optimum model and model parameterization schemes for the particular region of interest, and the consequent issues of stationarity and tuning. Consequently, most impacts assessments still rely on GCM results (which are not very skillful at the spatial scales required) for their principal source information on future climate possibilities. While some regional-scale information content can be crudely derived from GCMs (e.g. Hewitson, 2003), there is a continuing demand for robust downscaling techniques that reflect a regional climate manifestation inherently consistent with the large-scale, GCM-simulated response of the climate system dynamics to anthropogenic forcing.

GCMs now have a history of intercomparison studies (e.g. Lambert and Boer, 2001; Achuta Rao and Sperber, 2002; Covey *et al*., 2003) and there have been several recent initiatives to carry out similar studies for RCMs (e.g. Christensen *et al*., 2005). Although empirical downscaling algorithms can be broadly categorized into one of three or four major methodologies, there are varied implementations of these methodologies, and there has been little attempt at systematic intercomparison studies. Wilby *et al*. (1998) began the process by contrasting several techniques, but the comparisons, so far, have been limited in scope and have not addressed the broad spectrum of empirical techniques found in the literature. On the other hand, it could be argued that there is unlikely to be a 'best' downscaling algorithm, and that the optimum technique is likely to be application- and region specific. There may not be much to be gained by an in-depth intercomparison study, and it may be more important simply to clearly articulate the benefits and limitations of any particular downscaled product for the user community.

What we present here is a downscaling procedure that utilizes the commonly accepted advantages of several techniques, while minimizing their limitations. The objectives are to:

(1) Present a discussion of what constitutes a robust downscaling application. This builds on previous discussions in the literature beginning with Hewitson and Crane (1996), where questions over the selection of atmospheric predictors were explored, and continues more recently with the guidance documents on climate change scenarios published by the IPCC Task Group on Impact Assessments (Wilby *et al*., 2004).
(2) Develop a downscaling algorithm that seeks to address these issues and which, if not completely, then to some extent qualifies the remaining uncertainty. We suggest that this or similar approaches are required if the downscaled products are to be defensible, and of value to the policy and impacts communities.
(3) Apply the technique to a dense precipitation observational network in South Africa.
(4) Derive a range of precipitation statistics that can have immediate application in the formulation of adaptation and mitigation strategies in response to anthropogenic climate change in the region.

While assessing GCM performance was not a specific objective of the study, the results presented here suggest that much of the discrepancy between GCM projections of precipitation over South Africa (at least for the three models used here) may be due to differences in parameterization schemes, rather than inherent differences in the GCM simulations of regional dynamics.

2. EMPIRICAL DOWNSCALING: ISSUES OF CONCERN

Before presenting a new methodology, and in the light of the diversity of approaches that currently exist and the limited number of intercomparison studies, it is worth re-examining the basic principles and assumptions of empirical downscaling. This provides the context for explaining the particular approach adopted here. Empirical downscaling is conceptually very simple and is based on the premise that the local-scale climate is in some measure a response to the larger, synoptic-scale forcing. Observational data are used to derive a relationship between the synoptic-scale and local climates, and that relationship can then be used with comparable resolution fields of a GCM to generate information on the local climate consistent with the GCM forcing. The assumption that the local climate is conditioned by the larger-scale forcing is reasonable, even where the local climate is governed by mesoscale events such as convective systems, as these are, in turn, conditional on the synoptic state.

2.1. Synoptic-scale versus *local forcing*

While it is true that the synoptic-scale forcing will have some influence on local climate, there is also a degree of local forcing that will vary by region and by season. This local forcing can be both fixed and variable. Topography and land–water boundaries represent a fixed forcing for the local climate. The degree to which that forcing impacts the local climate, however, is also a function of the larger-scale flow. Consequently, the effects of this local forcing can be readily incorporated in the downscaling transfer function if appropriate measures of flow direction, stability, etc. are included in the predictor variables.

Variable local forcing would include, for example, land use and land cover change. For some regions, this could have a major impact on local climates, which cannot be captured by empirical downscaling techniques. While there have been sensitivity studies with both GCMs and RCMs that examine the impacts of land cover change (e.g. Taylor *et al*., 2002; Gao *et al*., 2003), we are not aware of any generally available RCMs that include two-way interactive vegetation or land cover schemes, or include scenarios of changes in land use practice. However, this is obviously something that should eventually be included in any RCM used for climate change impacts analysis. While impacts analyses can examine possible land cover/land use changes as one of a set of multiple stressors, the degree to which land cover changes can feedback to impact local climate represents an element of uncertainty in the climate projections analogous to, e.g. uncertainty due to future levels of greenhouse gas emissions.

In addition, for any synoptic state, there may be variation around a generalized response conditional on, for example, antecedent soil moisture. This small-scale variability is not captured by the GCM and the effects, therefore, are not included in the transfer function. Depending on the spatial scale involved, some of these may be treated explicitly by RCMs. For both empirical downscaling and for sub-grid-scale processes in RCMs these variations become a stochastic permutation of the response to a given synoptic state and can be modeled as such. Some downscaling methodologies are more appropriate for extracting the direct synoptic-scale forcing, while others are more effective at generating the stochastic element. At the same time, some techniques capture only the linear forcing, while others may capture any nonlinear forcing that may be present.

2.2. Stationarity

Given that there is a relationship between the larger-scale and the local climate, and assuming an appropriate downscaling transfer function can be generated, an empirical downscaling of present climate is eminently feasible. However, an additional factor becomes important when considering future climates – that of stationarity of the downscaling function. It is not immediately obvious that a relationship derived for the present climate can be applied to a future climate state. Empirical downscaling implicitly assumes that the observational data from which the relationship is developed encompasses the required information for future cross-scale relationships. Essentially, this assumes that, for a given region, the same synoptic-scale states are present in the future and that climate change will, for the most part, manifest itself as a change in the timing, persistence, and frequency of these larger-scale events. While we cannot verify stationarity until after the

fact, we can at least make some assessment of the likelihood on the basis of the changes in the large-scale climate of the GCM.

More difficult to assess is the possibility that the nature of the transfer function itself will change in the future. In many respects, appropriate selection of atmospheric variables that fully encompass the physics of the large-scale forcing would obviate this. However, if a change signal is present in a variable not selected, this can result in the transfer function progressively becoming less appropriate. One possible example would be if the concentration of cloud condensation nuclei significantly changes over a region. However, it is likely that such effects will be secondary to changes attributable to the core circulation and humidity attributes of the atmosphere. The degree to which this is likely to be an issue will also depend on the time scales considered (the further we project into the future the more likely this is to be an issue) and on the choice of predictor variables used.

2.3. Predictor variables

Past work (e.g. Hewitson and Crane, 1996; Cavazos and Hewitson, 2005) has shown that the choice of predictor variables is critical in capturing the anthropogenic climate change signal in the GCM. By using fields that reflect the primary circulation dynamics of the atmosphere, one captures part of the synoptic-scale forcing. Neglecting the inclusion of some measure of atmospheric humidity as a predictor, however, could have a notable effect on a downscaled climate change precipitation signal (see Hewitson and Crane, 1996; Crane and Hewitson, 1998). For a precipitation downscaling, including humidity not only improves the transfer function predictions for the present climate, but also reduces the stationarity issue noted above, as the dynamics and the humidity fields become separate predictors in the downscaling function. From this perspective, it is essential to have multiple predictor variables that have an understandable physical relationship to the downscaled parameter. Relationships that are purely correlative and for which there is no clear physical process linkage should be avoided. For example, the El Nino southern oscillation (ENSO)–Africa teleconnection that induces drought in southern Africa during El Niño (e.g. Rautenbach and Smith, 2001) has shown indications of weakening in recent years (Landman and Mason, 1999; Sewell and Landman, 2001). Consequently, there is no reason to expect that such teleconnection relationships will be maintained in future climates, and their use as predictors should be avoided.

2.4. Temporal resolution

A final issue is that of temporal resolution. Downscaling from time-mean fields is clearly feasible (see, for example, the discussion by Buishand *et al*., 2004). However, it is important to recognize that in some regions, climate change may be manifest as changes in the histogram of daily synoptic-scale events, with or without a change in the mean itself. Downscaling from time-averaged fields thus runs some risk of missing an important climate change signal.

In summary, the major issues to be addressed in any downscaling application should include:

(1) An assessment of the strength of the synoptic-scale forcing on any given variable for a given location – in other words, an assessment of the relative importance of synoptic-scale, local, and stochastic forcing, and of the degree to which the synoptic-scale forcing is linear *versus* nonlinear. In practice, this is most effectively accomplished through validation of the downscaling product. The degree to which the local climate of a test data set is reproduced by the downscaling function is an indication of the relative strengths of the large-scale *versus* local forcing.
(2) An assessment of the degree to which the future climate regime is reflected in the observational data used to generate the relationship (i.e. the stationarity issue).
(3) The use of predictors that reflect the physical processes controlling the local climate response.
(4) Downscaling at the time scale of daily weather events, even if these are to be subsequently aggregated in some fashion for impacts analysis.

In addition, the utility of the final product will also depend on the GCM(s) used for the analysis, the quality and duration of the observational network, and issues related to specific techniques (for example, assumptions

about data distributions that may be inherent in a particular statistical model). How all of these are addressed will affect the quality and the reliability of the downscaled climate projections. In some cases, this assessment process may indicate that a particular empirical downscaling approach is not viable for a region, application, or data set.

With these considerations in mind, we present a downscaling methodology that addresses each of these issues and produces an effective regional climate change scenario for South Africa, within the constraints of the degree to which the large-scale climate change is captured by the GCMs used.

3. SELF-ORGANIZING MAPS

A self-organizing map (SOM) is a data description and visualization tool that extracts and displays the major characteristics of the multidimensional data distribution function. SOMs are typically depicted as a two-dimensional array of nodes (although other topologies are possible), where each node is described by a vector representing the mean of the surrounding points in the multidimensional data space. In one respect, SOMs are similar to a 'fuzzy' clustering algorithm in which there are no distinct boundaries between groups, and individual data points can contribute to the definition of more than one group. In other applications SOMs can be thought of as being analogous to obliquely rotated nonlinear empirical orthogonal functions (EOFs) or in another sense, a projection of the n-dimensional data space onto a two-dimensional array of generalized modes. SOMs were introduced by Kohonen (1989, 1990, 1991, 1995), and examples in the literature include their potential applications to synoptic climatology (Hewitson and Crane, 2002), precipitation regimes (Crane and Hewitson, 2003), and interpolation schemes (Hewitson and Crane, 2005). SOMs were used by Malmgren and Winter (1999) and Cavazos (1999, 2000) for climate classification, by Hudson (1998) to examine synoptic circulation changes in GCM perturbation experiments, and by Ambroise *et al*. (2000) for cloud classification. Other related applications of SOMs are discussed in Cavazos and Hewitson (2005), Ni *et al*. (2002) and Tennant (2003).

The SOMs are derived from an iterative training procedure. The SOM is a user-specified, two-dimensional array of nodes, each defined by a reference vector of length n. For a $(n \times m)$ data set where n is the number of variables and m is the number of observations:

- We take the first observation and compare the observational vector to each of the node reference vectors in the SOM (typically using Euclidean distance as the measure of similarity). The reference vector that is closest to the observational vector is the 'winning node'. The reference vector of the winning node is then updated, adjusting it slightly in the direction of the observational vector by a user-determined factor that represents the 'learning rate'. Too large a learning rate may lead to an unstable solution, while a small learning rate takes longer to converge on a solution. In practice, we start with a relatively small learning rate and decrease it further with subsequent iterations. Given that the computational needs are very modest (compared to an RCM) we simply set a small learning rate and an arbitrarily large (500 000) number of iterations. Note that, unlike a feed-forward type of Artificial Neural Network, we are not fitting a function, and there is no issue of over-training or over-fitting with the SOM.
- All surrounding nodes are also updated, again being adjusted slightly (to a lesser degree than the winning node) in the direction of the observational vector. The radius of nodes around the winning node that are updated is determined by the 'update kernel' that decreases in radius during the iterative learning.
- Each observational vector is then presented to the SOM in turn and the procedure repeated for all of the observations.
- The process is then repeated for multiple iterations until there is no change in the node assignment of each observation between iterations.

Typically, we assign random values to the initial node vectors, although other options are available (e.g. using the first two principal components of the data set). We also use a two stage process whereby we start with a fairly large update kernel (close to the size of the smaller SOM dimension) for the first set of iterations.

Then using that final SOM as the starting point, we do a second training run with a smaller update kernel to refine the node definitions.

SOMs have some particularly advantageous characteristics from the point of view of climate downscaling:

- As noted above, each node reference vector is the n-dimensional mean of the nearby cloud of data points. The distribution of the SOM nodes in the data space is a function of data density and data similarity. The iterative training and the use of the update kernel result in similar observations mapping to nearby nodes, while observations that are very different to each other map to nodes that are located further apart in the SOM space. The SOM mapping, therefore, provides a simple and effective visualization of the n-dimensional (and possibly nonlinear) data structure.
- More nodes are, after training, located in areas with greater data densities, and fewer nodes where there are fewer data points. Because the update kernel adjusts surrounding nodes during the training process, it is possible that, if sufficient nodes are available (i.e. a large enough SOM), the SOM may also locate nodes in regions of the data space where there are no observations – in effect interpolating. The end result is that the SOM nodes represent archetypical points that span the continuum of the input data space.
- SOMs, unlike statistical models, make no assumptions about the underlying data, and the iterative training allows the SOM to describe any arbitrary linear or nonlinear data distribution function.
- The SOM is very effective at handling missing data in the observational vector. The comparison between the observational vector and the node reference vector is based on matching pairs of vector elements, and the SOM uses whichever pairs are available when computing the distance between the two vectors.
- The SOM gives consistent results regardless of the SOM dimensions used. The training procedure ensures that the most different patterns will move to opposite corners of the SOM array. As the array size increases, the same patterns are revealed, but with greater differentiation in the surrounding nodes. Large arrays present more detail in the pattern differentiations, while smaller arrays produce greater generalization – but the underlying structure remains the same (e.g. Crane and Hewitson, 2003).

4. SOM-BASED DOWNSCALING

In essence, using observational data we apply SOMs to characterize the atmospheric circulation on a localized domain around the target location, and we generate probability density functions (PDFs) for the rainfall distribution associated with each atmospheric state. For the downscaling we then take the GCM data, match it to the SOM characterization of the atmospheric states, and for each circulation state in the GCM data, randomly select precipitation values from the associated PDF. The general methodology is discussed in detail below.

4.1. Data

In this application we use daily mean atmospheric fields constructed from 6-hourly NCEP reanalysis data for 1979 to 2002, restricting the range to post-1979 when the advent of satellite data for the reanalysis significantly improved the quality of the reanalysis for the Southern Hemisphere (Tennant, 2004). The GCM data are from simulations using the CSIRO Mk2, ECHAM4.5, and HadAM3 (using sea-surface temperatures (SST) from HadCM3) GCMs models, forced by the SRES A2 emissions scenario. As the GCM data to be downscaled need to be of the same dimensions as the observational data, in this implementation the NCEP and GCM data are re-gridded to a common compromise grid of $3^\circ \times 3^\circ$. The data used to characterize the atmosphere are comparable to the boundary conditions used to force an RCM, and include the u and v wind vectors (surface and at 700 hPa), temperature (surface), specific humidity (surface and at 700 hPa), and relative humidity (surface and 700 hPa). Both relative and specific humidity are included, as the former reflects how close to saturation the atmosphere is, while the latter reflects the total water content.

A number of permutations of the mix of atmospheric variables and atmospheric levels were explored, and generally performed with comparable skill. Recognizing the high degree of correlation between variables and between levels in the atmosphere, the variables used here represent a common set that reflect the primary

circulation and water vapor attributes. As noted by Cavazos and Hewitson (2005), the most relevant generic variables that should be selected as the base predictors for downscaling are those of mid-troposphere circulation and humidity. In addition, we include the surface variable, as it has been noted that in regions in which orographic forcing plays a significant role, the surface data improve the characterization of the atmospheric states that differentiate between precipitation regimes.

The precipitation data used are from a high-resolution, gridded data set for South Africa described by Hewitson and Crane (2005). This data set has been created at both 0.1° and 0.25° resolutions from a source station observation data set of >3000 stations. The 0.25° resolution data set is used in this paper, as it is comparable to the resolution of RCMs used in climate change downscaling applications. The interpolation methodology used (conditional interpolation) explicitly uses synoptic conditioning of the interpolation parameters, and avoids or minimizes many of the problems inherent in interpolating a spatially discontinuous field such a precipitation.

The location of the precipitation data grid cells define the locations of the *downscaling targets*, the locations for which the atmospheric data are to be used to predict the local precipitation response.

4.2. The SOM procedure

A separate SOM is produced for each of the local 3×3 grids domains from the re-gridded atmospheric data. For each downscaling location, we take the 3×3 atmospheric grid ($\sim$1000 km $\times$1000 km) whose center cell is most co-located with the target downscaling location and train an SOM using the selected atmospheric variables to characterize the generalized daily atmospheric states. In this implementation, this means we are using the nine variables for each of the nine grid cells in the 3×3 window, creating an 81-element vector describing the atmospheric state. The time series consists of 24 years of daily data. The individual data fields are first standardized using the means and standard deviations of the 3×3 cell time series, thus preserving the local gradients in each field. These fields are then used to train an SOM of 9×11 nodes (allowing for 99 possible generalized atmospheric states, which, if the observations were equally distributed across the nodes, would lead to $\sim$90 observations defining the generalized state represented by any given node).

The training uses the two-step process described above, with 500 000 iterations for each training step. (Note: training an SOM is not vulnerable to over-training, as is perhaps the case with other techniques. The number of training iterations is chosen here to be overspecified.) Each day in the time series then uniquely maps to one of the trained 99 (from the 9×11 node array) different atmospheric states described by the SOM node vectors. This procedure is repeated for each 3×3 atmospheric grid, so that, for each downscaling location, there is a unique set of possible synoptic states described by its own spatially coincident local 3×3 grid cell climatology.

4.3. Determining a synoptically controlled precipitation PDF for each precipitation grid point

The downscaling is conducted at the resolution of the precipitation data set – in this case the 0.25° grid. For each location in the precipitation grid, we take the most closely co-located 3×3 atmospheric grid and its related SOM. For each SOM node, we take all of the days that map to that node and subset the related daily precipitation. The objective is to develop a precipitation PDF for each SOM node. We do this by:

(1) Rank-ordering the precipitation observations for the node. We simply list all the precipitation occurrences from low to high – including all the days with zero precipitation.
(2) Fitting a spline to the ranked data to give a continuous function.
(3) Interpolating off the spline to M ranks (typically 100). We take the spline curve and divide it into 100 equal units in order to account for the fact that the nodes may have differing numbers of observations. These interpolated rainfall values are equivalent to the PDF for that SOM node. There is no need to explicitly compute a PDF, as later we sample the 'PDF' using a random number generator to select a precipitation value from one of the 100 cells.
(4) Repeating this procedure for all nodes in the SOM.
(5) Repeating for all target precipitation grid cells.

Every target precipitation location is thus described by 99 different PDFs related to the 99 generalized atmospheric states in the SOM for that location.

4.4. Downscaling

We take the same atmospheric window and atmospheric variables that we used to train the SOM and extract these from the GCM data. We then standardize the GCM data using the same procedure as we used with the NCEP data. For the GCM simulation data of future climate, we standardize using means and standard deviations of the simulation data for the present-day climate, hence preserving any changes in the future from the present-day means and standard deviations. We then map these data to the already trained SOM, and find the node to which each atmospheric state of the GCM maps. In other words, for every atmospheric domain coincident with a given target location, we have an SOM that describes the synoptic states associated with that domain as derived from observational data, and we have mapped the daily atmospheric states of the GCM control and future climate simulation data onto the same set of observed synoptic states.

For a given atmospheric domain, we can also examine the number of days that map to each of the SOM nodes (i.e. number of times a specific atmospheric state occurs) for the observed climate, the model control climate, and the model projection of future climate. Comparing the frequency counts, and the error function in mapping the different atmospheric fields to the SOM, for the observed (NCEP) climate and the model control run gives a measure of model validation – it gives a first indication of how well the control run matches the distribution of atmospheric states as seen in the NCEP reanalysis data ('observations'). Comparing the frequency and mapping error across the SOM nodes for the GCM control and future climate simulations demonstrates whether the climate change GCM nominally spans the states represented in the NCEP/control run data. If a significant portion of the climate change data shift to one edge of the SOM, or if the mapping error significantly increases, this could indicate a lack of stationarity. An example is discussed later in the paper.

To downscale the precipitation data we take each target location and associated SOM of atmospheric states. For the SOM node to which a particular day maps, we can then determine a precipitation value by randomly selecting from the associated PDF generated in the earlier step. A random number generator is used to select a value (r) between zero and one, which is then multiplied by M (number of ranks extracted from the spline of the PDF) to select where on the PDF to read the precipitation amount. This approach works reasonably well; it generates rainfall events of the correct magnitude, but slightly underestimates the number of rainy days in regions of higher rainfall. For these regions, there is some degree of temporal autocorrelation that is not completely captured by this approach. Some persistence is included through the dependence on the synoptic state. However, a given state does not always produce rainfall – a factor that is accounted for by the PDF – but if a given state produces rainfall on day 1, it is more likely that a similar state will produce rainfall on the next day as well. The degree of persistence varies for each grid cell and for each synoptic state. It probably varies by season and may not be the same for a future climate state. For this reason, we account for persistence by modifying r (the random number generator). If rainfall occurs on day 1, then for day 2 we use the $\sqrt{r}$ generated for day 2. Using $\sqrt{r}$ nudges the selection slightly toward the wetter end of the PDF. For many atmospheric states rainfall occurs only in the top portion of the PDF, and thus using $\sqrt{r}$ does not have a large impact. However, it does increase the persistence slightly in the wet areas without the need to explicitly calculate persistence for every individual data point and time period. In validating the downscaling, it appears this simple adjustment provides appropriate compensation for persistence.

Once the rainfall value has been extracted, we continue to generate the full time series (daily data for the length of record being used) and repeat this 100 times. That is, we produce 100 time series with slight variations due to the random selections from the PDFs, but where each record is still constrained by the same larger-scale atmospheric controls. For each of these 100 records we calculate monthly precipitation statistics including:

(1) Number of rain days.
(2) Number of rain days with greater than 2 mm rainfall.

(3) Number of rain days with greater than 20 mm rainfall.
(4) Total rainfall in the month.

Other statistics, such as the 90th percentile rainfall event and the mean and median dry spell duration could also be developed if needed.

For each month we determine the mean, median, and standard deviation of the above statistics across the 100 time series of monthly statistics, thus generating a monthly time series that reflects the median and mean responses within the stochastic envelope. The standard deviations present a measure of variability that is due to the sub-grid-scale stochastic contribution to precipitation at any target location, where the stochastic contribution has been conditioned by the larger-scale forcing. Finally, we take the monthly time series with the closest match to the median monthly time series of the iterations, and save the daily form of this as a representative time series of daily values.

5. APPLICATION TO SOUTH AFRICA

5.1. Downscaling from reanalysis data

While 24 years of NCEP reanalysis data are available to develop the SOMs, the precipitation data set ends in 1999. Figure 1 thus shows the downscaling applied to 21 years of daily NCEP data from 1979 to 1999. The observed annual total and the annual totals predicted by the downscaling from the atmospheric data demonstrate a close match in both magnitude and spatial distribution. Figure 2 shows a comparison of the observed and downscaled data in terms of the number of rain days per month in winter and summer, and demonstrates that the downscaling captures the seasonal differences, the spatial gradients across the country, and the high orographic rainfall region of the Drakensberg Mountains in the southeast. The downscaling also captures the summer convective systems in the interior plateau, as well as the winter frontal rainfall over Southwest Cape. Of particular interest is the downscaling's ability to capture the sharp gradients along the southern coast.

Figure 3 shows that the downscaling is not highly dependent on the specific years of the time series used, so long as enough data is present in order to define the shape of the PDF for each synoptic state. The top panel shows the results when the complete record is included in the training, the middle panel shows the results when eight years, selected at random, are excluded, and the bottom panel shows the differences of the two. The small differences are an indication of the robustness of the solution. While the downscaling can capture only synoptic states that are present in this 21-year period, the technique is not particularly sensitive to the specific years used.

To explore the degree of local stochastic *versus* synoptic forcing, Figure 4 picks one target location in the summer convective rainfall region (26 °S; 28 °E) and shows the median time series of monthly mean totals over 6 years, along with the one standard deviation envelope of the 150 realizations of downscaling conducted for this target. The figure shows how the downscaling captures the interannual variability, and indicates how wide the stochastic envelope is, demonstrating how the degree of stochastic control is seasonally dependant. In this case, we see that for this summer rainfall region, as one might expect, the stochastic component increases for summer months when rainfall is a product of convective processes.

5.2. Assessment of GCM circulation

Before examining the downscaled climate change from the GCMs, it is valuable to first consider the changes in atmospheric circulation projected by the GCMs, and how this relates to the issue of stationarity. Figure 5 takes a downscaling target location – one in the summer convective regime on the interior plateau, and explores the frequency attributes of the associated 3×3 cell atmospheric predictor window.

Figure 5 shows the frequency of days mapped to each of the SOM nodes for the NCEP data, by contouring the frequency across the 9×11 node array. Each node has an associated reference vector, representing the generalized atmospheric state. These generalized atmospheric states could be plotted as nine figures (one for

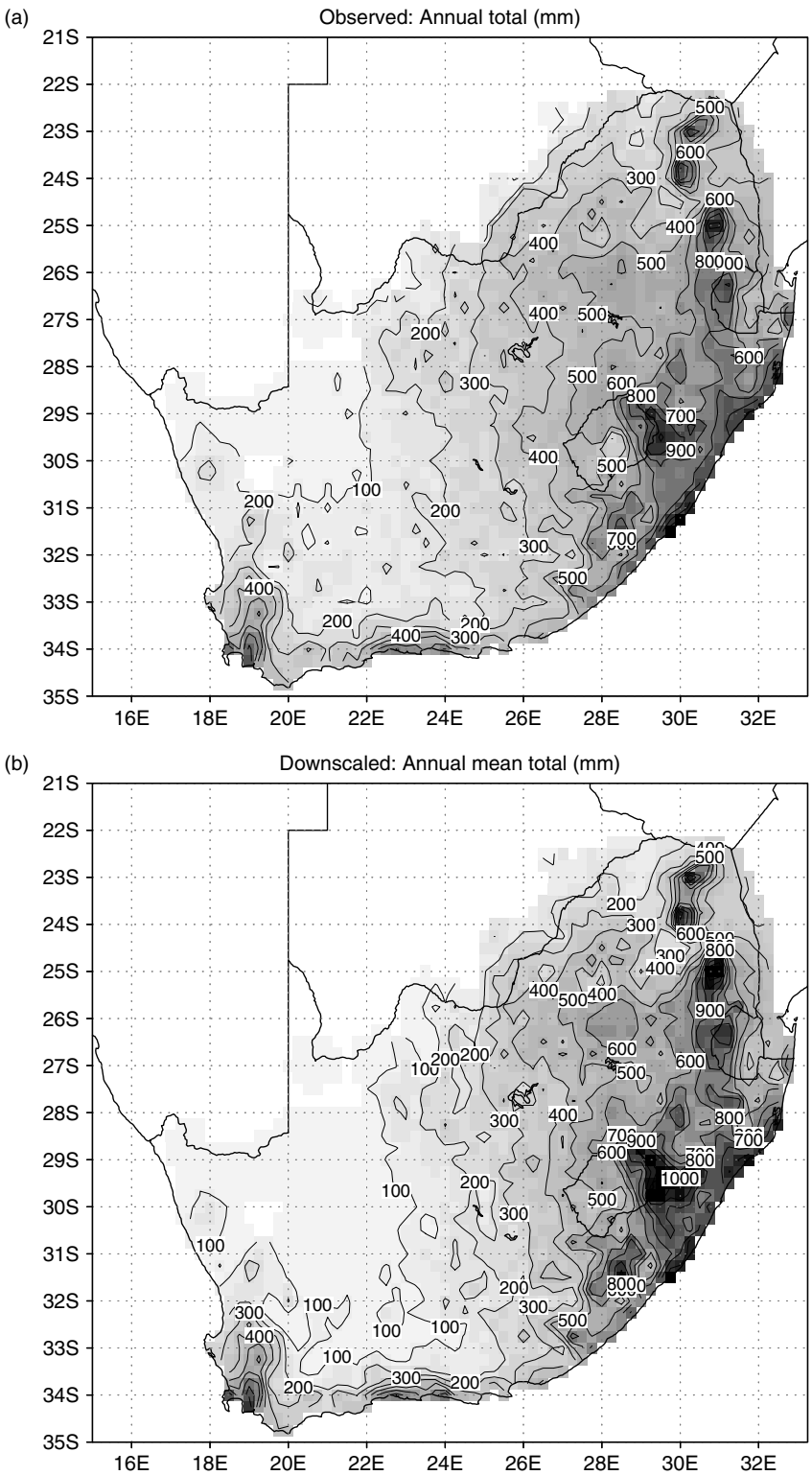

Figure 1. Mean annual total precipitation (mm). Observed mean precipitation totals (a) from gridded station precipitation (Hewitson and Crane, 2005), and empirically downscaled precipitation (b) from NCEP atmospheric circulation fields, for the period 1979–1999

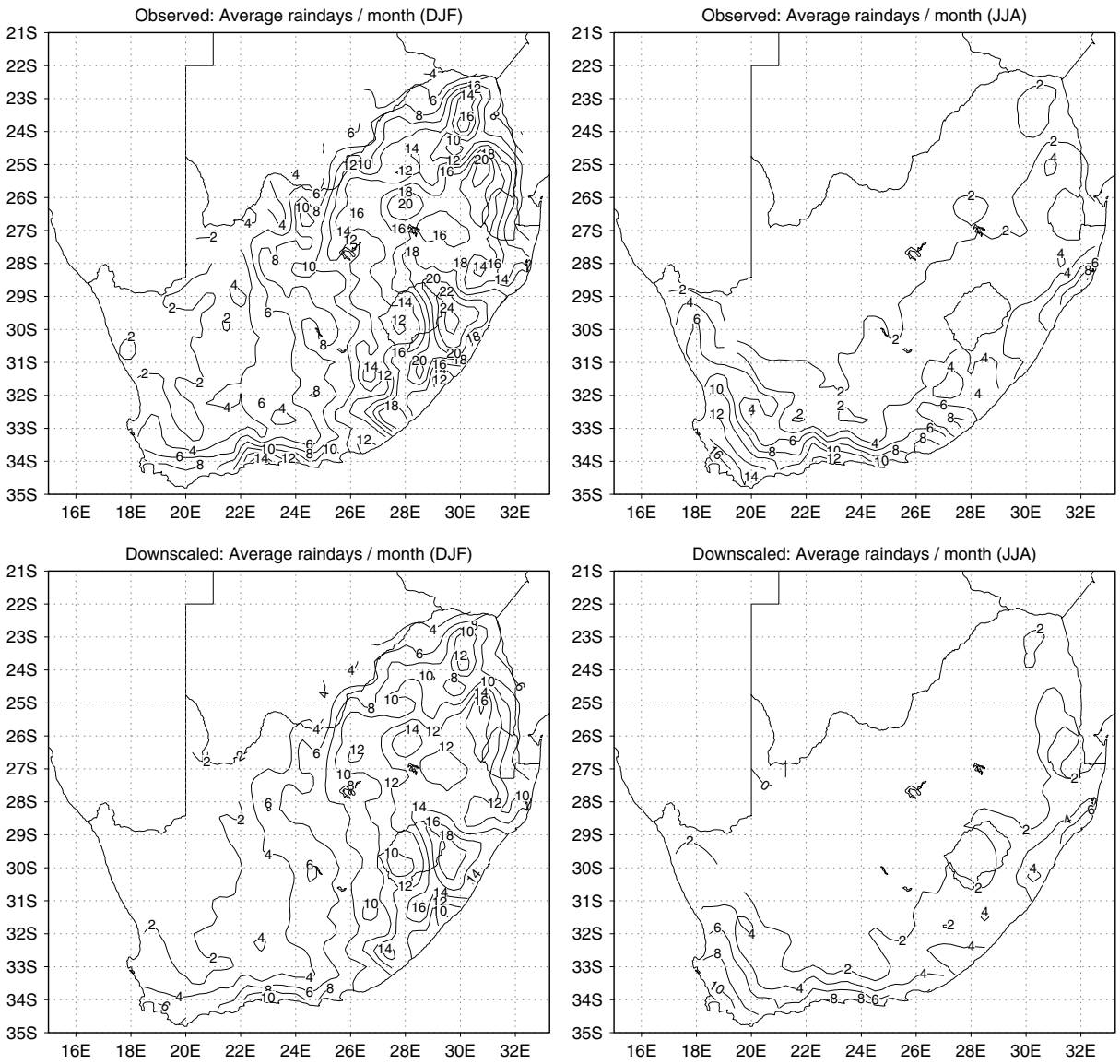

Figure 2. Mean number of rain days per month for summer (December, January, February (DJF) – left panels) and winter (June, July, August (JJA) – right panels) observed (top) and empirically downscaled (bottom), for the period 1979–1999

each variable), where each figure would consist of a matrix of 9×11 maps. To save space, these are not presented here (see Hewitson and Crane, 2002, for an example of a SOM node mapping of synoptic pressure fields). The NCEP map shows the distribution of occurrence of atmospheric states, in effect a two-dimensional histogram. As is common with SOMs, the centers of high frequency are located near the edges and corners of the map (Hewitson and Crane, 2002).

The remainder of Figure 5 shows, in each column, the results for each of three GCMs: the HadAM3, the ECHAM4.5, and the CSIRO9 Mk2. Given that the GCMs are being mapped to an SOM already trained by the NCEP data, one could anticipate several possible outcomes. If the GCM data map to the SOM nodes with a frequency distribution very similar to the NCEP data, it would indicate that the GCM has the same synoptic-scale structure and temporal behavior as the observed climate. Alternatively, the GCM could map to the SOM with a very different frequency distribution, indicating some differences in the temporal characteristics of the

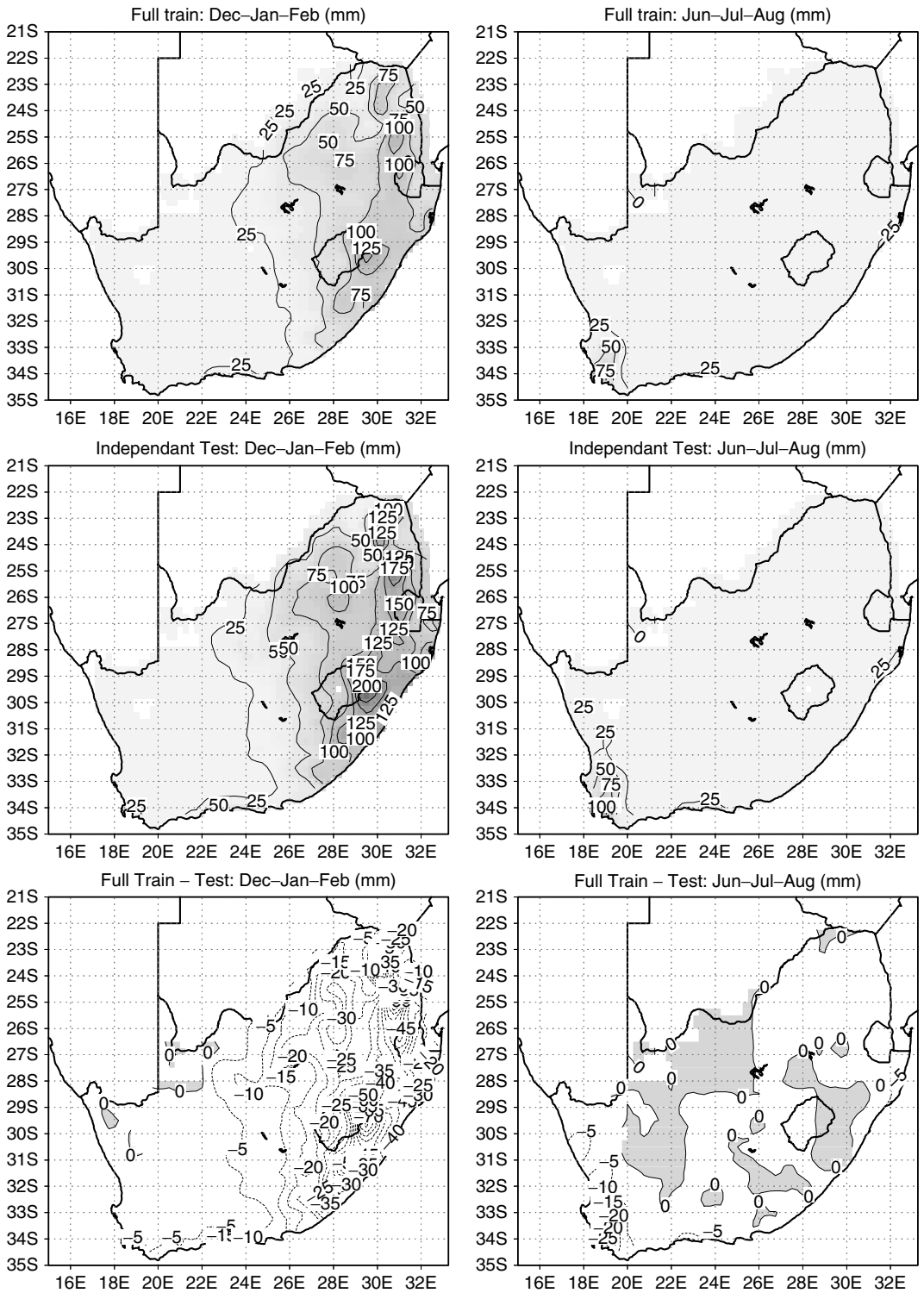

Figure 3. Comparison of downscaled mean monthly precipitation (mm) for summer (DJF – left panels) and winter (JJA – right panels) over eight random years when using the full record from 1979 to 2002 to train the downscaling, or a partial record. The top panels are the downscaled precipitation for the eight random years from the SOMs trained with the full record. The middle panels are the downscaled precipitation for the 8 years when these years are excluded from the training of the SOMs. The lower panels show the anomaly between the two

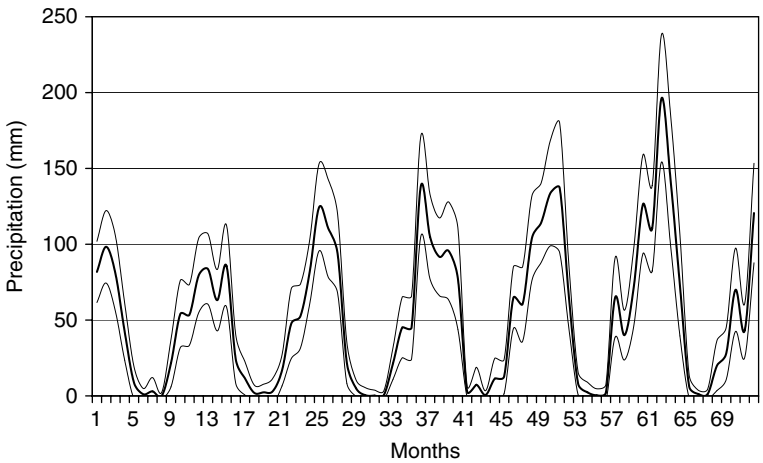

Figure 4. Sample of 6 years of monthly precipitation (thick line), bounded by 1 standard deviation of the 150 downscaled series for these years. The downscaled data are for a summer rainfall location. The graph demonstrates that the degree of stochastic variability varies seasonally, yet the downscaled data captures the large scaled circulation forcing of both the intra- and interannual variability

circulation. If the frequencies clustered in one section of the map, it would indicate a substantial difference between the observed and modeled atmospheres, with a large portion of the model atmospheric states most likely lying outside of the SOM domain. Focusing on the top row of Figure 5 (the frequency distribution across the nodes for the GCM control simulation of present-day climate) it is apparent that the GCMs have distributions similar to that of NCEP, but with higher frequencies centered on fewer nodes – suggesting that the modeled climate represents a reduced dimensionality and lower variability system compared to the observed climate. Note, however, that the models generally occupy the same feature space as the observed (NCEP) climate. However, the models all show a preference for different atmospheric modes, revealing a mode bias that varies between GCMs.

The second row of Figure 5 shows the frequency distribution of the simulated future climates, in general showing a similar distribution to the control runs. Nodes that had high frequency counts in the control run have even higher counts in the future climate, and day-to-day variability is further reduced. The bottom row of the figure shows the anomaly of frequency change. While the frequency distribution of daily circulation states from the control run shows differences between models, and each model has different bias compared to the NCEP frequency distribution, the models' climate change circulation anomalies show marked similarities between GCMs. This suggests that while the models have unique bias, the dynamic response to anthropogenic greenhouse gas forcing is comparable. Given that the precipitation fields from GCM climate change projections often show marked disagreement between GCMs (see later), this commonality of dynamic circulation response suggests that the climate change signal can be coherent between models: that perhaps the parameterization of diagnostic variables such as precipitation is a significant contributor to the intermodel differences in projections of precipitation change. If this is the case, empirical downscaling as presented here potentially can expose a more robust climate change signal between multiple GCMs – given that it is based on the spatial nature of the dynamic circulation response.

Figure 6 expands on the examination of GCM circulation and explores more explicitly the issue of stationarity. Each node reference vector represents a mean state for a subregion of the data space, as discussed earlier. When observations are mapped to a given node of the SOM, there is an error factor: a measure of the degree to which the node reference vector exactly represents the observation vector. As the data are standardized, the values are standardized units, and represent the mean absolute error of the comparison of data vector with the reference vector, giving an indication of the variability of observations mapping to a given node.

Plotted in Figure 6 is the mean error with which the NCEP atmospheric states map to each node. For the most part the error is consistent across the nodes, indicating the nodes effectively represent the span of the data

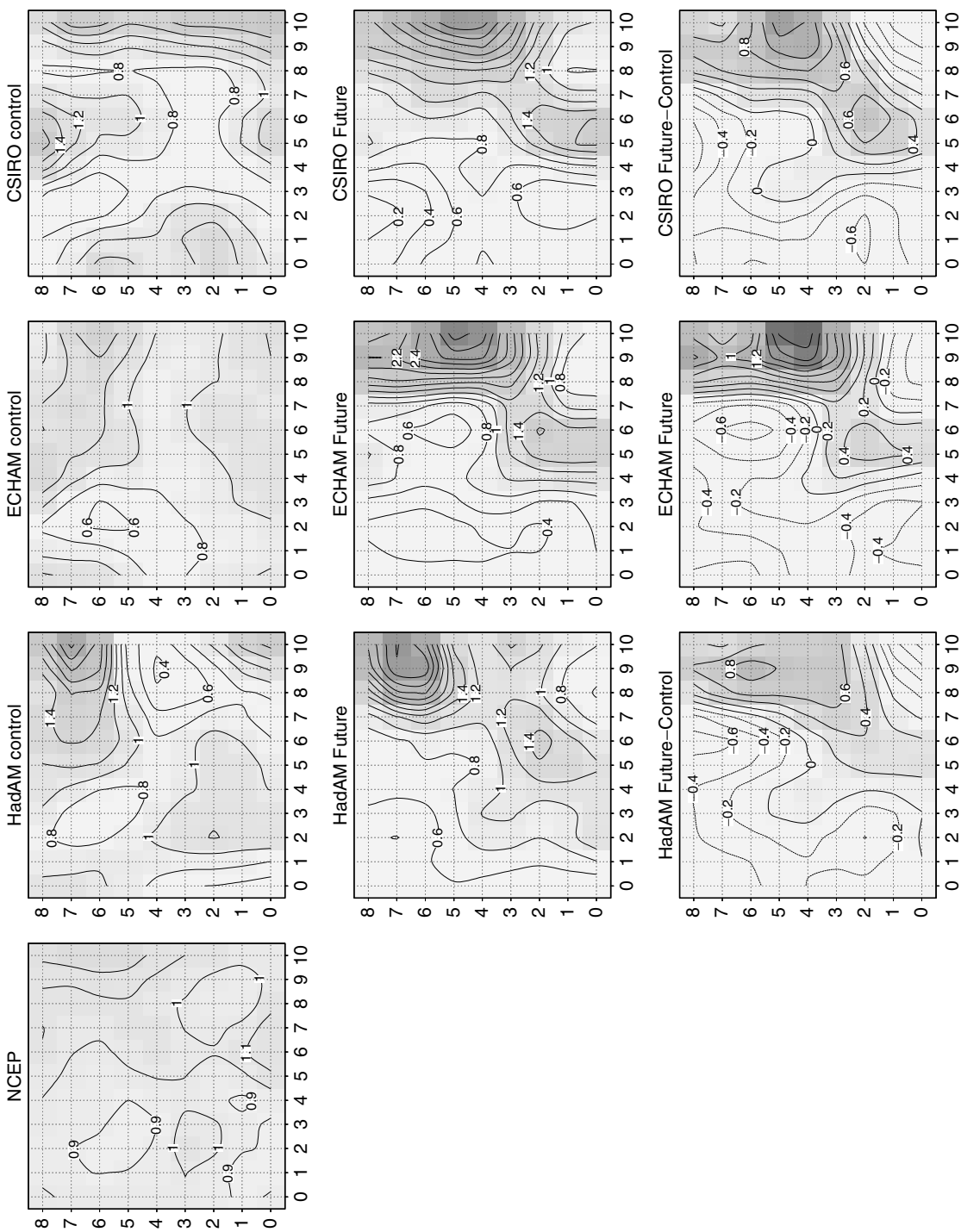

Figure 5. Frequency distribution across the SOM nodes for atmospheric circulation centered on 26 °S and 28 °E. The top row shows the frequency plot for circulation fields in the NCEP reanalysis data, and in the control period simulation data of the three GCMs. The middle row shows the frequency distribution for the future climate as simulated by the three GCMs. The lowest row shows the frequency anomaly between the future and control climate simulations for the three GCMs

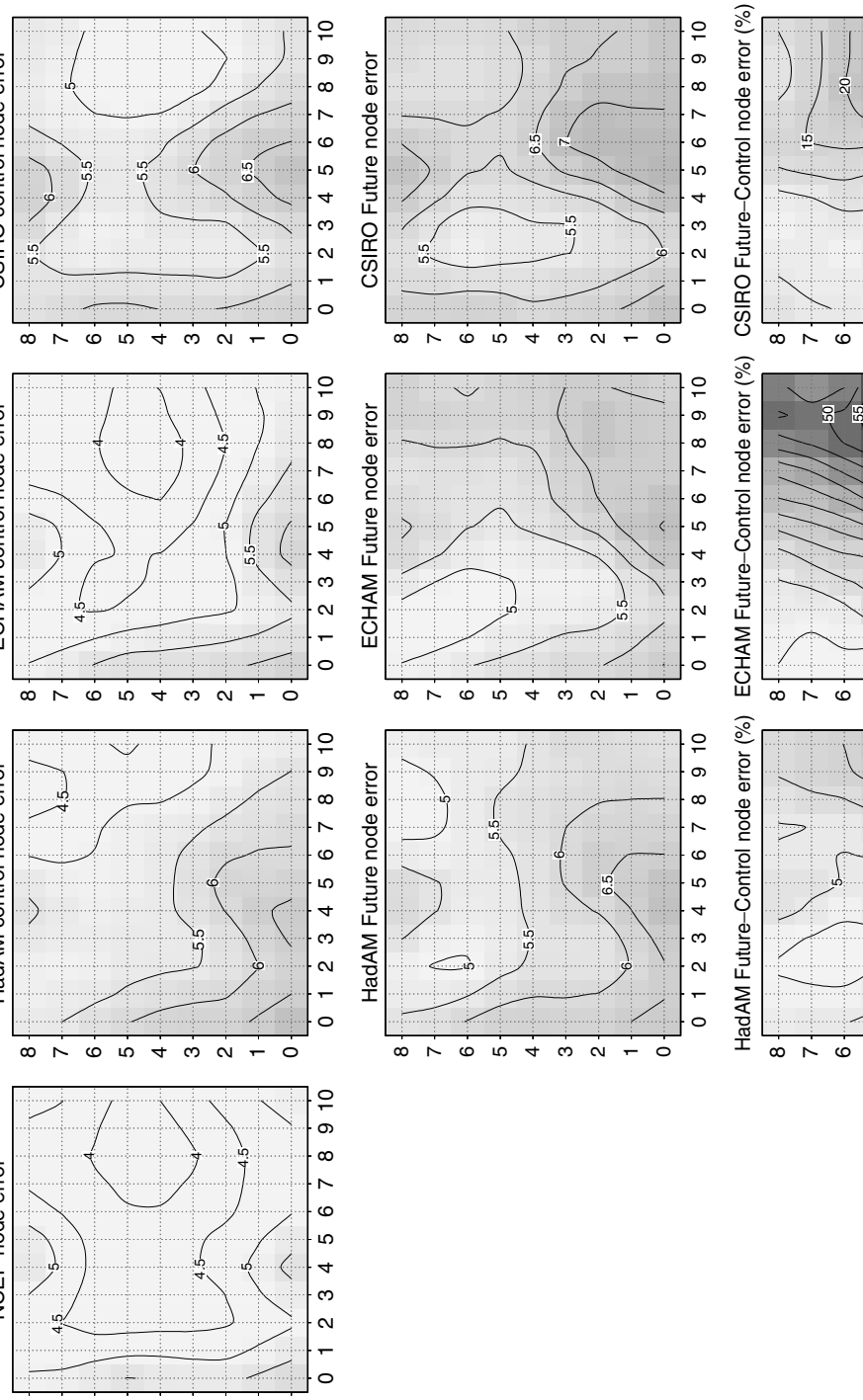

Figure 6. Mean node error of days mapping to the SOM nodes for atmospheric circulation centered on 26 °S and 28 °E. The top row shows the node error for circulation fields in the NCEP reanalysis data, and in the control period simulation data of the three GCMs. The middle row shows the node errors for the future climate as simulated by the three GCMs when mapped to the SOM. The lowest row shows the percent change in the node error between the future and control climate simulations for the three GCMs, where the magnitude of the change is indicative of the degree to which future synoptic states exceed the envelope of the control climate

across the n-dimensional data space. The remainder of panels in the top row of Figure 6 indicates the node error for the GCM control simulations, with the second row showing the node error from the simulations of the future climate. The mapping of the GCM data to the nodes show increased error over the NCEP data – indicating that the GCMs simulate circulation states that, although representing similar atmospheric states to the NCEP data, have some degree of disparity and bias. It is possible to investigate this further by examining the atmospheric states of the nodes in which the GCM data are most deviant from the NCEP defined states, and so understand which dynamic processes in the model are less well simulated. However, such analysis is beyond the scope of this paper.

The lowest row of Figure 6 is the change in the error factor between the GCM control and future simulation data. Two attributes are of note here: first that, as in Figure 5, the model-simulated change between the control and future climate again shows remarkable agreement between GCMs. This supports the earlier suggestion that there is a robust change signal between GCMs in terms of the circulation dynamics. More relevant with reference to stationarity, is the degree to which the error of the future climate mapping to the SOM nodes exceeds the error of the control run data. It is clear that the future simulation data show an increase in the mapping error, indicating a measure of non-stationarity in the circulation. A way to consider this is to understand that the control simulation data define an envelope of the climate. The future simulation similarly has a climate envelope; however, there is a non-perfect overlap of the two climate envelopes – the climate envelope has shifted. The anomaly node error plots of Figure 6 are thus a measure of the GCM's data stationarity. For the most part, the non-stationarity component of the future climate is relatively small; most nodes have changes in mapping error in the range of 0–20%. A few nodes show moderate growth in non-stationarity, with some nodes, in particular with the ECHAM model, having a change of up to 60%.

On one level, the stationarity issue is a potential problem, especially if one were using a transfer function between the circulation and the precipitation based on, for example, some form of linear or nonlinear regression. However, in the case of the SOM downscaling, the procedure is inherently conservative. If a future climate data sample fell outside of the envelope of climate defined by the data used to train the SOM, the data sample would then be mapped back to the node that is closest within the n-dimensional data space. By selecting rainfall amounts from these nodes, we have a conservative estimate of the future climate response and, at worst, we underestimate the change.

In light of this conservative attribute of the downscaling in the presence of non-stationarity, the procedure provides a robust means to downscale the climate change signal. For example, dominant anticyclonic systems over a region may increase beyond the intensity of present-day climate. However, in such a situation the downscaling would still reflect a local climate response of a dominant anticyclonic system, only for that of a less intense system.

5.3. Downscaled climate change

The downscaled precipitation needs to be viewed in the light of what the GCM parameterized precipitation indicates. Figure 7 shows typical GCM climate change anomalies for precipitation, contoured in terms of the change in mean annual precipitation – the magnitudes of the anomaly reflect a 10–15% change. Notable is the disagreement between the three GCMs; CSIRO-Mk2 shows a decrease over effectively the whole domain while the ECHAM4.5 and HadAM3 show drying in most of the domain, with increases over the eastern portion, although disagreeing in the spatial extent and magnitude of the increase. Note, these GCM precipitation fields are from the IPCC DDC (Data distribution center. See http://ipcc-ddc.cru.uea.ac.uk/) archive of monthly mean values for these models, as the daily precipitation data for the models were not available for this study. Nonetheless, the results are reflective of the typical GCM consensus (or lack thereof).

One way of using the GCM precipitation information in Figure 7 would be to present an average of the three maps, or to present the differences between the maps as a measure of uncertainty – to provide high and low bounds for a climate scenario. Both approaches are problematic. This is not simply a case of different estimates of the magnitude of the change or a slight phase shift or offset in the location of some controlling feature (such as storm tracks, etc.). These are not three variations of a similar climate response, and averaging the three makes very little sense. If the models are simulating precipitation accurately, these could represent

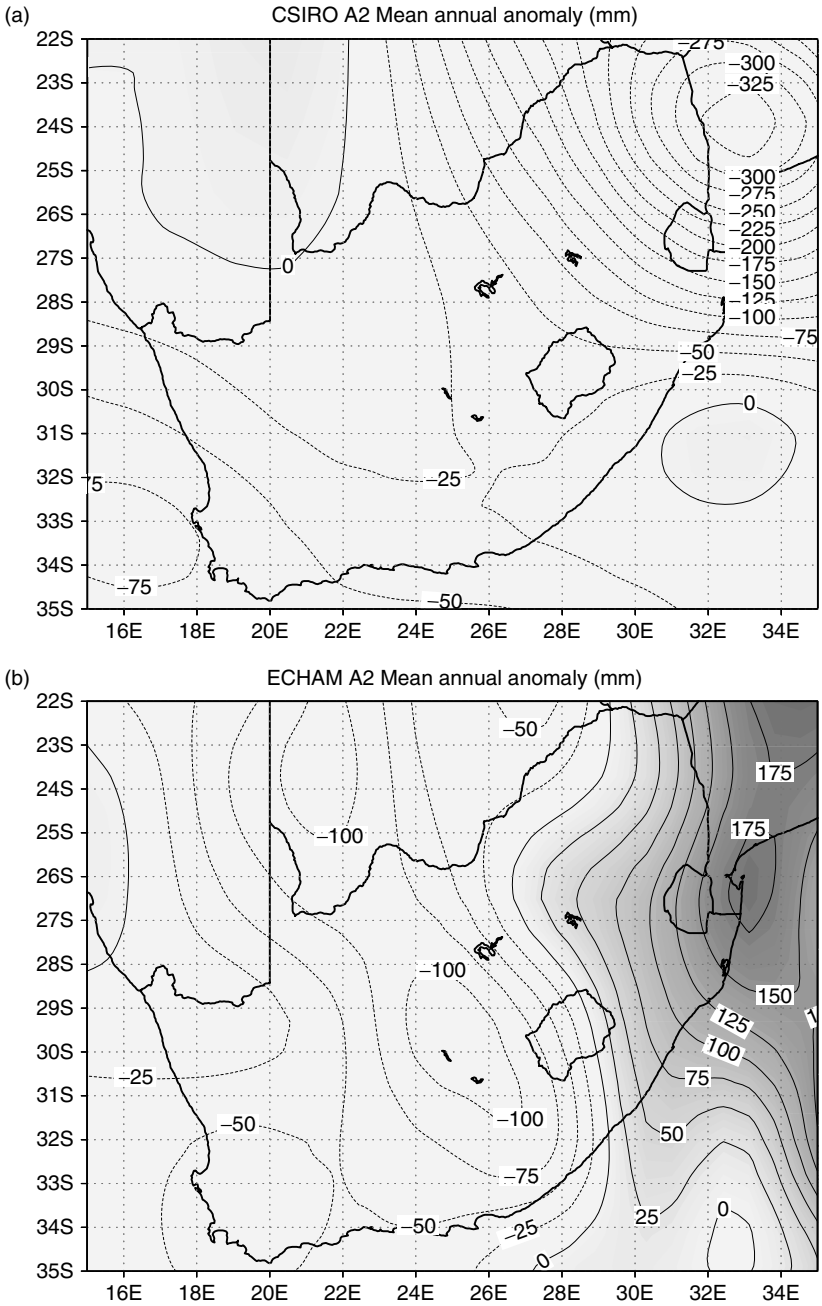

Figure 7. Projected climate change anomaly in mean annual precipitation from three GCMs

three equally possible responses to the same forcing, and the differences could be regarded as a measure of uncertainty in the climate system. However, if the differences are due to differences in the precipitation parameterization schemes and their interaction with the model dynamics (or the model topography, land surface climatology, etc.), then the three maps represent more a measure of uncertainty in our ability to effectively simulate the climate system over this region. Either way, the differences in sign, spatial patterns, and anomaly gradients across the region indicate that the GCM precipitation fields provide little information that would be beneficial for impacts assessment.

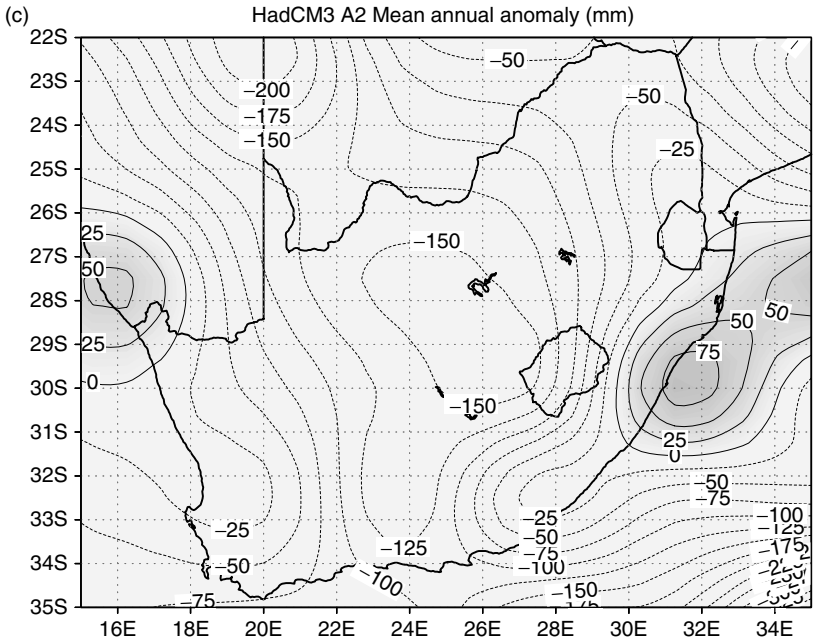

Figure 7. (*Continued*)

The downscaling results present a very different picture. Figure 8 shows the climate change anomaly from differencing the downscaled control and future daily atmospheric data of the three GCMs. Two facts are of immediate note: the downscaling provides regional detail that is consistent with the actual spatial gradients over the region, and the pattern agreements of positive and negative changes are remarkably consistent across the three GCMs. This general agreement in the direction and spatial distribution of the changes is in marked contrast to Figure 7. The most likely explanation is that all the models capture the larger-scale forcing reasonably well, and all of them project similar changes in atmospheric state for this region. Consequently, the downscaled results show similar distributions, which would also suggest that much of the difference in Figure 7 is due to differences in the way the models derive their precipitation values, rather than disagreements over their projection of future atmospheric circulation. This same consistency is seen in Figure 9, which shows changes in the number of rain days, and Figure 10, which shows changes in the number of days with a rainfall over 20 mm. The ECHAM4.5 forced downscaling shows a far stronger downscaled response than the other two models, and reflects the concentration of the circulation change toward a (wet) subset of synoptic modes as shown in Figure 5.

Two localized regions of disagreement are: first, the mild winter increase in precipitation over the southwest corner of South Africa by the HadAM3 model, in contrast to the drying in the other two models, and second, the mild increase over the northern border in summer shown by the ECHAM4.5 model, whereas the other two models indicate drying. However, in the latter case, the ECHAM4.5 model already appears to be far too wet in summer, and this may result in the model atmospheric states over the northern border not reflecting the drying as seen in the other two models.

As noted earlier, since the downscaling generates daily data, it is possible to calculate a number of relevant statistics about the attributes of the daily precipitation. In Figures 9 and 10 we show the climate change anomaly in the number of rain days with precipitation greater than 2 mm and greater than 20 mm (heavy rainfall days). These are parameters of particular significance for hydrology and water resources, as well as agriculture. At the same time, this is a difficult parameter to estimate from GCMs, as the GCM grid cells tend to precipitate on most days, being a large area average parameter. The downscaled rain day anomalies track the spatial changes in rainfall totals to a fair degree, but not completely, in some cases showing a decrease in rain days where totals increase, or vice versa, and indicating that there are changes in intensity as well.

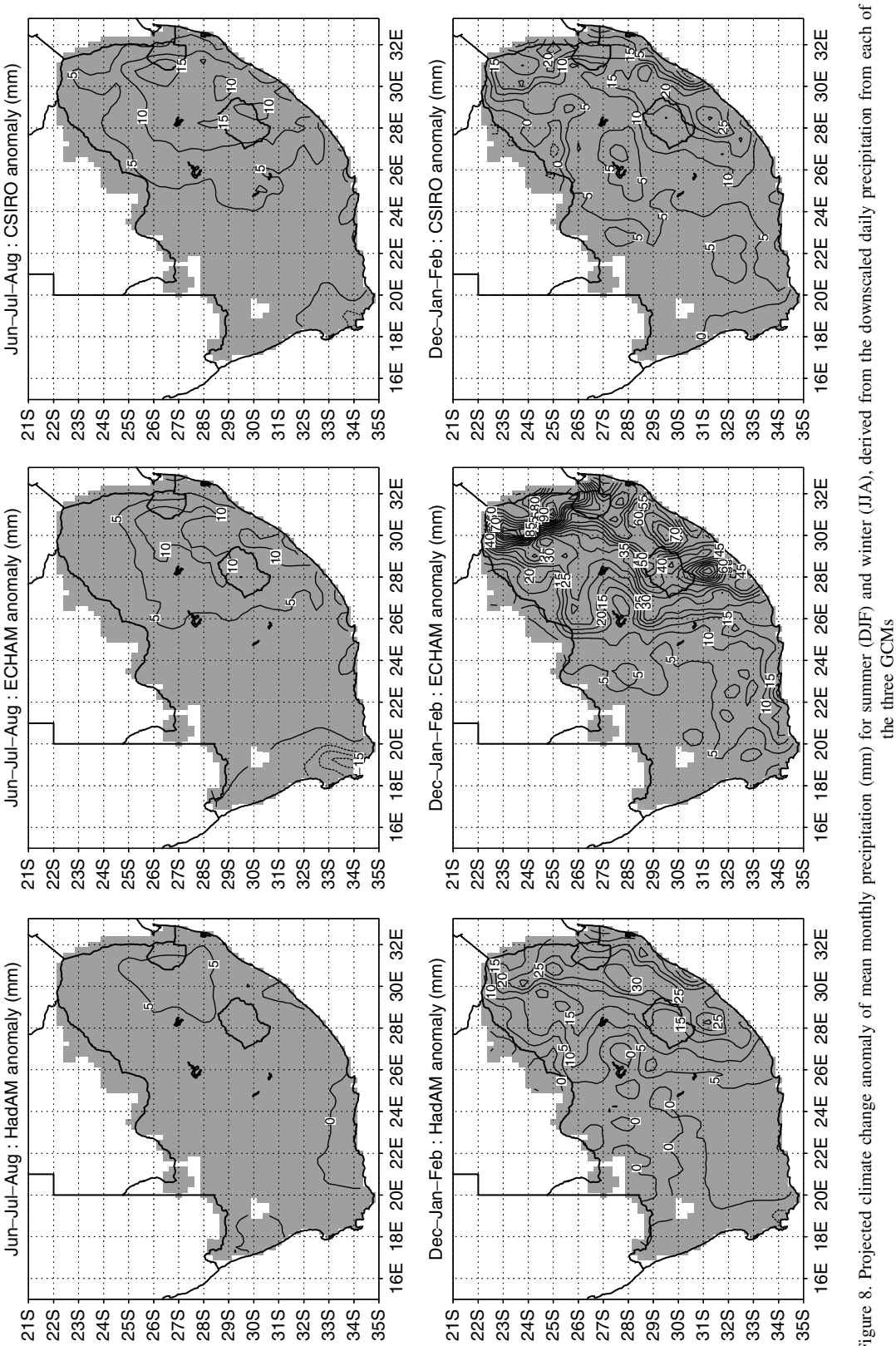

Figure 8. Projected climate change anomaly of mean monthly precipitation (mm) for summer (DJF) and winter (JJA), derived from the downscaled daily precipitation from each of the three GCMs

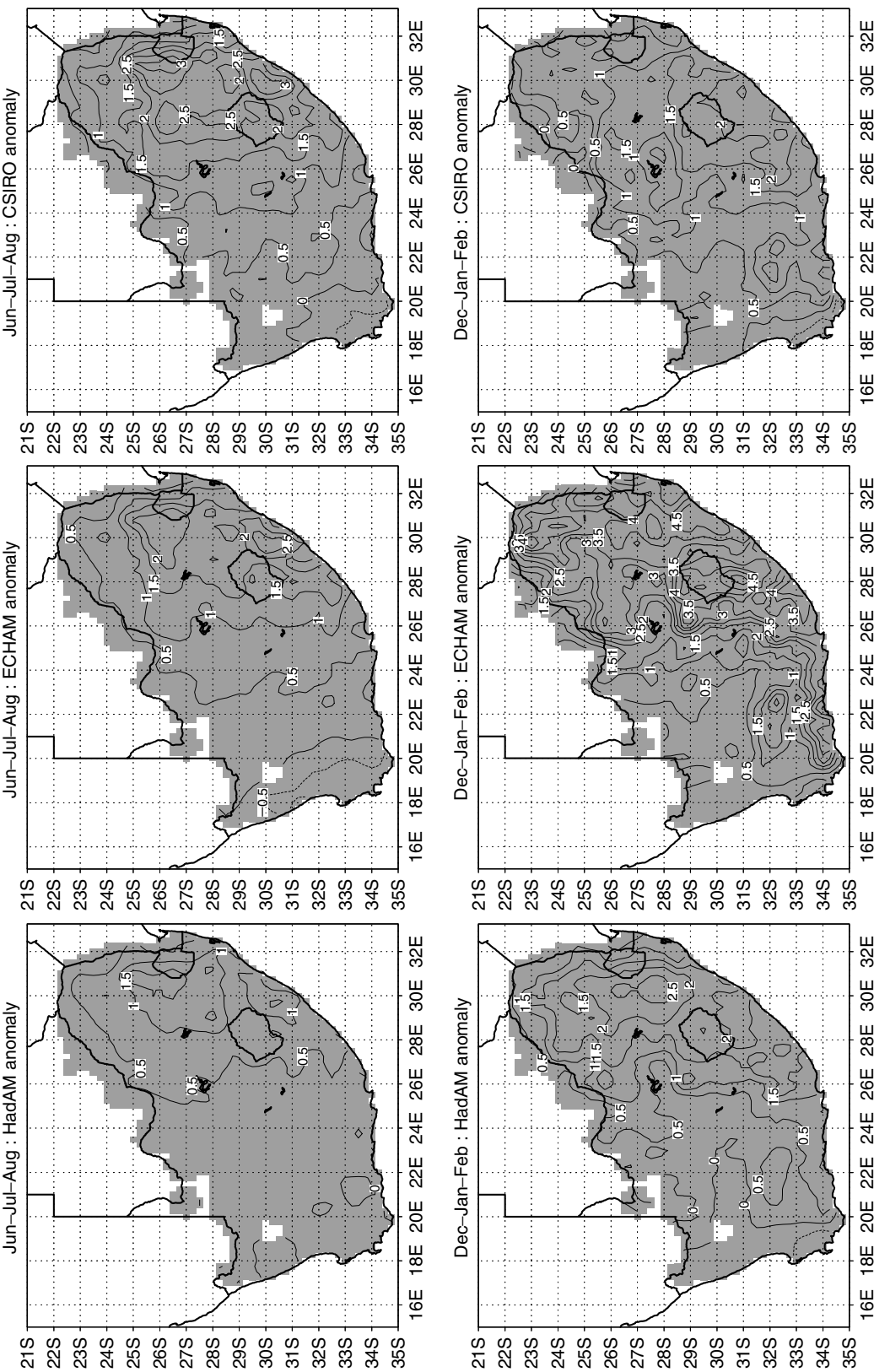

Figure 9. Projected climate change anomaly of the mean number of rain days per month for summer (DJF) and winter (JJA), derived from the downscaled daily precipitation from each of the three GCMs

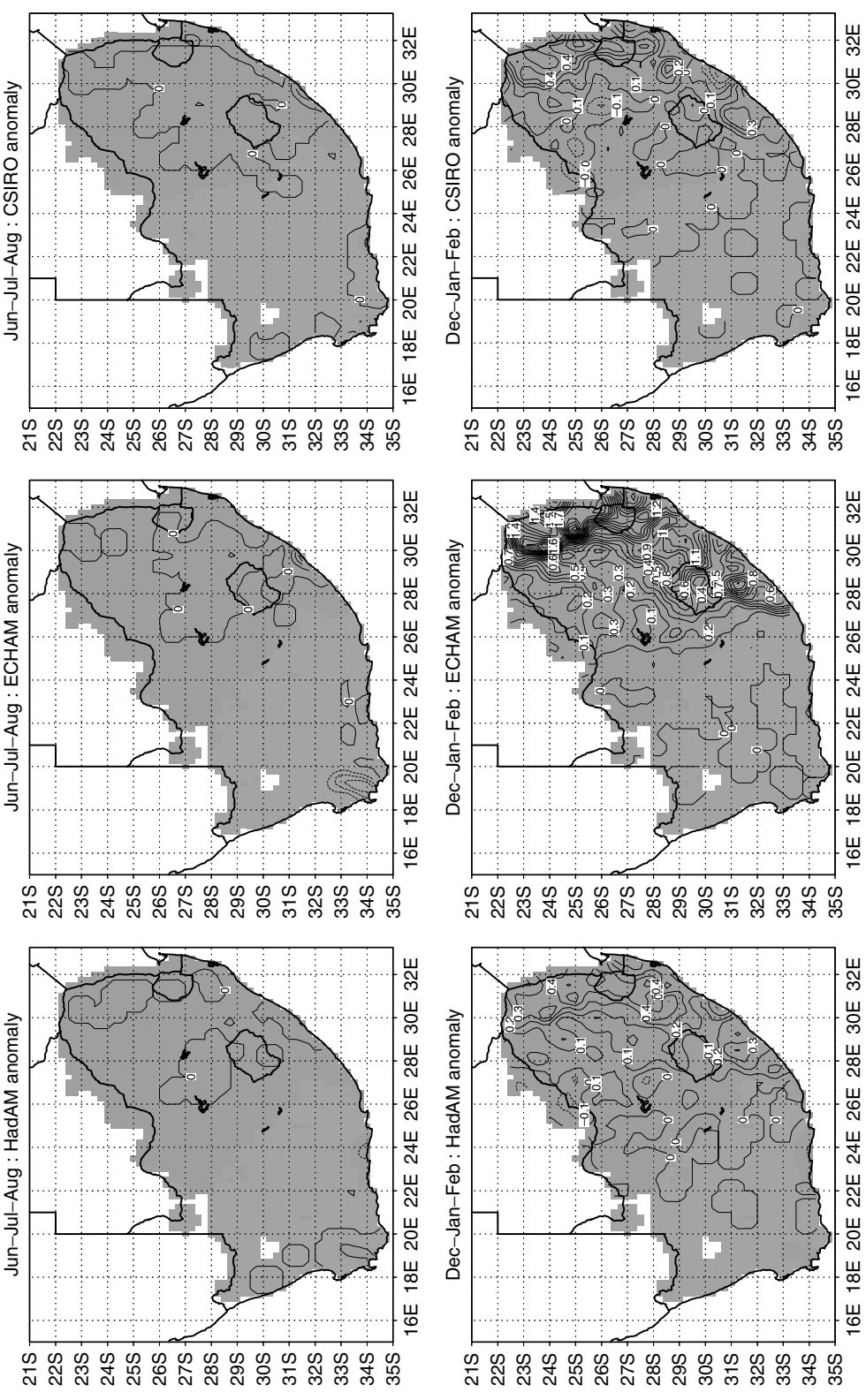

Figure 10. Projected climate change anomaly of heavy rainfall events (rain days > 20 mm) per month for summer (DJF) and winter (JJA), derived from the downscaled daily precipitation from each of the three GCMs

6. SUMMARY AND DISCUSSION

The development of regional climate change scenarios has been subject to debate, with the outcomes dependant on the GCM employed, the downscaling method used, and the assumptions involved. With the improvement in GCM skill, and the convergence in the circulation response to greenhouse gas forcing between GCMs, the opportunity exists to develop regional-scale scenarios of future change that are inherently consistent with the GCM forcing. The methodology presented here offers an inexpensive solution that may be quickly employed with a broad range of GCM outputs, and one that is inherently conservative in the presence of non-stationarity in the climate system. The downscaled solutions for South Africa show notable coherency when forced by several different GCMs; the magnitudes of projected change differ, but the spatial pattern of the change is largely in agreement. The results indicate that South Africa will experience increased summer rainfall over the convective region of the central and eastern plateau and the Drakensberg Mountains. The Western Cape will see little change, with some slight drying in summer and a slight decrease in wintertime frontal rainfall.

Questions remain around the probability of occurrence of any one emission scenario over another, and the relative value of the empirically downscaled projection *versus* that which may be derived from RCMs. The first question is complex and, with current resources and data availability, is perhaps best approached through downscaling a range of GCM simulations forced with different, yet defensible, scenarios of future greenhouse gas emissions. In this respect, empirical downscaling is particularly advantageous in terms of computational efficiency. However, while the empirical techniques give a first-order response to the regional climate change that is physically consistent with the circulation, they are not capable of incorporating local-scale feedbacks. RCMs, on the other hand, are able to accommodate such feedbacks, but it is arguable whether this provides any greater confidence in the downscaled solution, given the significant sensitivity of the RCM to choice of parameterization schemes and physics packages. The selection of an empirical or modeling approach is likely to be determined by the resources available and the specific study objectives. The present results point to the potential for empirical techniques to demonstrate the convergence of different climate change projections from multiple GCMs. At the same time, they present an economical way of assessing a range of climate change scenarios: results that could be extremely useful from the policy and planning perspective. Numerical RCMs, however, are essential for assessing the potential impacts of multiple forcing factors (e.g. global climate and regional land use change).

In conclusion, it would appear that spatially cohesive projections of regional climate change are possible, where the changes are consistent with the GCM forcing, coherent in pattern across different GCMs, and defensible in terms of our understanding of the physical processes underpinning the change. The methodology implemented here is robust, conservative against stationarity, and readily implemented across multiple GCMs with minimal computation requirement.

REFERENCES

AchutaRao K, Sperber KR. 2002. Simulation of the El Nino Southern oscillation: Results from the coupled model intercomparison project. *Climate Dynamics* **19**: 191–209.

Ambroise C, Seze G, Badran F, Thiria S. 2000. Hierarchical clustering of self-organizing maps for cloud classification. *Neurocomputing* **30**: 47–52.

Buishand TA, Shabalova MV, Brandsma T. 2004. On the choice of the temporal aggregation level for statistical downscaling of precipitation. *Journal of Climate* **17**(9): 1816–1827.

Cavazos T. 1999. Large-scale circulation anomalies conducive to extreme events and simulation of daily precipitation in northeastern Mexico and southeastern Texas. *Journal of Climate* **12**: 1506–1523.

Cavazos T. 2000. Using self-organizing maps to investigate extreme events: An application to wintertime precipitation in the Balkans. *Journal of Climate* **13**: 1718–1732.

Cavazos T, Hewitson BC. 2005. Performance of NCEP variables in statistical downscaling of daily precipitation. *Climate Research* **28**: 95–107.

Christensen JH, *et al*. 2005. Evaluation of the performance and utility of regional climate models in climate change research: Reducing uncertainties in climate change projections–the PRUDENCE approach. *Climatic Change* [In Press].

Covey C, AchutaRao KM, Cubasch U, Jones P, Lambert SJ, Mann ME, Phillips TJ, Taylor KE. 2003. An overview of results from the coupled model intercomparison project. *Global and Planetary Change* **37**: 103–133.

Crane RG, Hewitson BC. 1998. CO2 precipitation changes for the Susquehanna basin: Downscaling from the GENESIS general circulation model. *International Journal of Climatology* **18**: 65–76.

Crane RG, Hewitson BC. 2003. Clustering and upscaling of station precipitation records to regional patterns using self-organizing maps (SOMs). *Climate Research* **25**: 95–107.

Gao XJ, Luo Y, Lin WT, Zhao ZC, Giorgi F. 2003. Simulation of effects of landuse change on climate in China by a regional climate model. *Advances in Atmospheric Sciences* **20**: 583–592.
Hewitson BC. 2003. Developing perturbations for climate change impact assessment. *EOS* **84**: 337–348.
Hewitson BC, Crane RG. 1996. Climate downscaling techniques and applications. *Climate Research* **7**: 85–95.
Hewitson BC, Crane RG. 2002. Self organizing maps: Applications to synoptic climatology. *Climate Research* **22**: 13–26.
Hewitson BC, Crane RG. 2005. Gridded area-averaged daily precipitation via conditional interpolation. *Journal of Climate* **18**: 41–57.
Hudson DA, 1998. Antarctic sea ice extent, Southern Hemisphere circulation and South African rainfall, PhD Thesis, University of Cape Town: South Africa.
IPCC (Intergovernmental Panel on Climate Change). Houghton JJ, Ding Y, Griggs DJ, Noguer M, van der Linden PJ, Dai X, Maskell K, Johnson CA (eds). 2001. *IPCC Working Group I*, Cambridge University Press: Cambridge, p. 881.
Kohonen T. 1989. *Self-Organization and Associative Memory*, 3rd edn. Springer-Verlag: Heidelberg.
Kohonen T. 1990. The self-organizing map. *Proceedings of the IEEE* **78**: 1464–1480.
Kohonen T. 1991. Self-organizing maps: optimization approaches. In *Proceedings of the International Conference on Artificial Neural Networks*, Espoo, Finland, June 1991, 981–990.
Kohonen T. 1995. *Self-Organizing Maps*. Springer-Verlag: Heidelberg.
Lambert SJ, Boer GJ. 2001. CMIP1 evaluation and intercomparison of coupled climate models. *Climate Dynamics* **17**: 83–106.
Landman W, Mason S. 1999. Change in the association between Indian Ocean sea-surface temperatures and summer rainfall over South Africa and Namibia. *International Journal of Climatology* **19**(13): 1477–1492.
Malmgren BA, Winter A. 1999. Climate zonation in Puerto Rico based on principal components analysis and an artificial neural network. *Journal of Climate* **12**: 977–985.
Ni F, Cavazos T, Hughes MK, Comrie AC, Funkhouser G. 2002. Cool season precipitation in the Southwestern United States since AD 1000: Comparison of linear and nonlinear techniques for reconstruction. *International Journal of Climatology* **22**(13): 1645–1662.
Rautenbach C, Smith I. 2001. Teleconnections between global sea-surface temperatures and the interannual variability of observed and model simulated rainfall over southern Africa. *Journal of Hydrology* **254**(1–4): 1–15.
Sewell R, Landman W. 2001. Indo-Pacific relationships in terms of sea-surface temperature variations. *International Journal of Climatology* **21**(12): 1515–1528.
Tennant W. 2003. An assessment of intraseasonal variability from 13-yr GCM simulations. *Monthly Weather Review* **131**(9): 1975–1991.
Tennant W. 2004. Considerations when using pre-1979 NCEP/NCAR reanalyses in the southern hemisphere. *Geophysical Research Letters* **31**: L11112, DOI:10.1029/2004GL019751.
Taylor CM, Lambin EF, Stephane N, Harding RJ, Essery RJH. 2002. The influence of land use change on climate in the Sahel. *Journal of Climate* **15**: 3615–3629.
Wilby RL, Charles SP, Zorita E, Timbal B, Whetton P, Mearns LO. 2004. *Guidelines for Use of Climate Scenarios Developed from Statistical Downscaling Methods*. IPCC Task Group on Data and Scenario Support for Impact and Climate Analysis (TGICA): http://ipcc-ddc.cru.uea.ac.uk/guidelines/index.html.
Wilby RL, Wigley TML, Conway D, Jones PD, Hewitson BC, Main J, Wilks DS. 1998. Statistical downscaling of general circulation model output: A comparison of methods. *Water Resources Research* **34**: 2995–3008.

